BOLETIN DE LA SOCIEDAD ESPAÑOLA DE
Cerámica y Vidrio
www.elsevier.es/bsecv

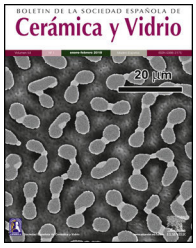

Production of vitreous materials from mineral coal bottom ash to minimize the pollution resulting from the waste generated by the thermoelectrical industry

Camila da Silva Gonçalves[a,*], *Adriano Michael Bernardin*[b], *Rozineide Aparecida Antunes Boca Santa*[a], *Cassio Leoni*[a], *Geraldo Jorge Mayer Martins*[a], *Claudia Terezinha Kniess*[c], *Humberto Gracher Riella*[a]

[a] *Chemical Engineering Department, Santa Catarina Federal University, P. O. Box 476, Trindade, 88.040-900 Florianópolis, SC, Brazil*
[b] *Santa Catarina Extreme South University, 88.806-000 Criciúma, SC, Brazil*
[c] *University Nove de Julho, 05001-000 São Paulo, SP, Brazil*

ARTICLE INFO

Article history:
Received 26 June 2017
Accepted 24 October 2017
Available online 23 November 2017

Keywords:
Mineral coal
Solid waste
Bottom ash
Pollution
Glasses

ABSTRACT

Mineral coal bottom ash exerts a great impact on the environment due to the presence of heavy metals in its composition and the lack of an adequate area for disposal. Vitreous materials were synthesized from bottom ash to be employed as a by-product. The bottom ash was subjected to an X-ray fluorescence (XRF) analysis to evaluate the oxide composition present in the material. To study the effect of bottom ash in the attainment of glass, a simplex lattice design for experiments with blends was employed. The elements considered in the design were: bottom ash; sodium carbonate (Na_2CO_3) and calcium oxide (CaO), both used as melting agents; magnesium oxide (MgO), which was used as a stabilizer for the vitreous network. For the characterization of the glasses, X-ray diffraction (XRD), differential scanning calorimetry (DSC) and Fourier transform infrared spectrometry (FTIR) were carried out. Ten different formulations were tested. The results indicated that two out of the ten formulations formed a crystalline phase, which is undesirable for a vitreous material. In the statistical analyses, the Pareto Diagram and the response surface showed that the glass transition and softening temperatures were strongly influenced by the level of calcium oxide and magnesium oxide, as well as that of bottom ash, resulting in an increase in the softening and glass transition temperatures.

* *Corresponding author.*
E-mail address: goncalvesscamila@gmail.com (C.d.S. Gonçalves).
https://doi.org/10.1016/j.bsecv.2017.10.007

Producción de materiales vítreos a partir de escoria de carbón mineral para reducir la contaminación producida por los residuos generados por la industria termoeléctrica

Palabras clave:
Carbón mineral
Desechos sólidos
Escoria
Contaminación
Vidrios

RESUMEN

La escoria de carbón mineral afecta profundamente al medio ambiente por la existencia de metales pesados en su composición y la falta de un área adecuada para su eliminación. Los materiales vítreos se sintetizaron a partir de escoria para ser empleados como subproducto. La escoria se sometió a un análisis de fluorescencia de rayos X (XRF) para evaluar la composición de óxido presente en el material. Para estudiar el efecto de la escoria en la obtención de vidrio, se empleó un diseño de malla simple para experimentos con mezclas. Los elementos que se valoraron en el diseño fueron: escoria; carbonato de sodio (Na_2CO_3) y óxido de calcio (CaO), ambos utilizados como agentes de fusión; óxido de magnesio (MgO), que se utilizó como estabilizador de la red vítrea. Para la caracterización de los vidrios se llevaron a cabo difracción de rayos X (XRD), calorimetría de barrido diferencial (DSC) y espectrometría de infrarrojos por transformada de Fourier (FTIR). Se probaron 10 formulaciones diferentes. Los resultados indicaron que 2 de las 10 formulaciones formaron una fase cristalina, que es indeseable para un material vítreo. En los análisis estadísticos, el diagrama de Pareto y la superficie de respuesta mostraron que la transición vítrea y las temperaturas de reblandecimiento estaban muy influidas por el nivel de óxido de calcio y de óxido de magnesio, así como por el de escoria, lo que aumentaba las temperaturas de reblandecimiento y transición vítrea.

Introduction

The coal-based thermoelectrical energy sector is an activity with large impact on the environment [1]. Mineral coal is one of the most employed resources throughout the world for energy production. Despite being a potentially polluting fuel, coal will probably continue leading as a source of energy generation [1]. According to the International Energy Agency and the World Coal Association [2], the combustion of mineral coal currently contributes with about 30% of the global primary energetic needs. The current coal reserves are estimated to be enough to meet the global production for approximately 150 years [2,3].

A crucial problem presented by mineral coal in thermoelectric is the generation of industrial waste, among which are tons of bottom ash and fly ash [4]. Fly ash are particles which move with the combustion gas as it leaves the furnace, while bottom ash are the particles which sediment at the furnace's bottom [5]. Bottom ash is considered one of the main industrial by-products [6]. The growing generation of ashes has long been source of environmental, technological and economic problems around the world [7]. According to data from the American Coal Ash Association (ACAA), in 2014 approximately 12 million tons of bottom ash were produced, and only 12% of those were subsequently used [8]. Given this context, the low frequency of utilization of this residue justifies the scarce existing research on the use of bottom ash [9].

Most technical and environmental problems associated with the use of mineral coal arise due to its inorganic components, especially the non-combustible ones [10]. According to Kim [11], the composition of bottom ash is basically constituted of SiO_2 (53.5%), Al_2O_3 (23.9%) and an acidic/basic oxides ratio of 2:1. The composition of the two ashes is practically the same, but the bottom ashes have more moisture [8], and larger particle size. According to Ulusoy and Igathinathane [12], particle size distribution is an important measurement of the physical characteristics of ash, exerting influence in various aspects concerning its utilization, such as heat and mass transfer, as well as homogeneity of its mixture with other components.

In this context, this research was elaborated to evaluate the potential of bottom ash obtained in the south region of Santa Catarina, Brazil, to be used as the main raw material in the production of glasses, thus minimizing the environmental impacts and obtaining new materials with added value. An experimental design for mixtures was utilized to constitute 10 glasses using sodium carbonate and a 2:1 mixture of CaO/MgO, respectively, as melting agents. The effects of each component in the thermal properties of the glasses were determined.

The sodium-calcium glasses were prioritized for this study because they comprise 90% of all glass produced on Planet Earth [13], that is, the demand for these materials is extremely high.

The large proportions of SiO_2 found in bottom ash form the glass phase, and the alumina (Al_2O_3) acts as an intermediate cation, making the chemical bond more stable with oxygen, increasing the viscosity of the medium and acting as modifiers when the medium is favorable [14].

Few researches are available on the application of bottom ash in the production of glasses. Choi and Kang [15], for instance, investigated the degree of surface crystallization and the crystallization mechanism for SiO_2–Al_2O_3–Li_2O glasses containing coal bottom ash. Kim and Kang [16] studied TiO_2 additions on the crystallization kinetics of a coal bottom ash Li_2O glass system. The main publications found with

Table 1 – Experimental formulation for 100 g of glass sample.

Samples	BA	Na_2CO_3	CaO/MgO
1	78.0	25.0	7.3
2	58.5	58.4	7.3
3	53.3	22.8	33.3
4	65.0	47.3	7.3
5	61.1	23.5	25.2
6	55.0	33.9	25.2
7	71.5	36.1	7.3
8	69.3	24.2	16.5
9	56.7	45.8	16.5
10	63.0	35.0	16.5

bottom ash are pertaining to ceramic and glass ceramic materials, cements, composites, among others. Contrastingly, this study deals with the synthesis and characterization of a material that is little explored in terms of publications.

Experimental procedure

Ash preparation

To withdraw moisture and facilitate its milling, bottom ash went through oven drying at 105 °C for 24 h. After the drying stage, the bottom ash was milled in a ball mill, model CS-501 K, for 24 h under a rotation of 65 rpm and with alumina balls of 10, 14 and 17 mm.

To identify the oxides present in the material, a gray sample was collected for X-ray fluorescence analysis (XRF).

Preparation of the formulations

For the preparation of the formulations an experimental planning for mixtures, simplex-lattice type, was employed. Bottom ash, being an industrial waste and presenting a large composition, was considered a pseudo-component. CaO and MgO melting agents were used in the ratio of 2:1, respectively. Na_2CO_3 was used as the source of Na_2O, and the loss of CO_2 during melting was taken into account in the calculation of the proportions, as shown in Table 1. The melting agents employed have a high degree of analytical purity.

The resulting glasses were annealed at a temperature of 5 °C above the T_g for 4 h, then cooled slowly to room temperature. Characterization analyses were performed under the annealed glass.

Table 1 shows the experimental formulation for a 100 g glass sample.

Fusion for the acquisition of the glass samples

The formulations were melted in a Schally oven (model LAB – S 5.6) at a temperature between 1480 and 1500 °C utilizing alumina crucibles, with volume of 70 mL. The crucibles containing each mixture were inserted in the oven, where they remained for 4 h until the complete fusion of the components, with a maximum melting temperature varying between 1480 and 1500 °C. At the end of the 4 h, the contents in the crucibles were poured in a metallic mold for the attainment of glasses.

Table 2 – Composition in oxides of the bottom ash under study.

Oxide	(% mass)
SiO_2	53.3
Al_2O_3	22.9
Fe_2O_3	15.1
K_2O	3.1
CaO	2.1
TiO_2	1.3
MgO	0.7
Na_2O	0.5
MnO	0.1
P_2O_5	0.1
Loss to fire	0.5

Characterization techniques

To identify the presence of crystalline phases, the X-ray diffraction (XRD) technique was employed. The analyses were performed via the powder method in a Philips X'Pert diffractometer with CuK α, radiation (1.5418 Å). The parameters of the analysis were: acceleration of 40 kV and 30 mA, 2θ interval of 3 to 118° and a step of 0.02° s^{-1}. The JCPDS database was utilized for the identification of the samples.

To characterize the mineral coal bottom ash, the X-ray fluorescence (XRF) technique, model Philips PW2400, was employed. For the execution of the assay, a bottom ash sample was pressed in a double layer with a base of boric acid, H_3BO_3 (Merck base), with a pressure of 5 tons for 10 s in a tablet shape. The tablet was then analyzed in an X-ray fluorescence spectrophotometer with a wavelength dispersion sensor (WDS).

The glasses underwent thermal analysis through the differential scanning calorimetry (DSC/TG) technique. The device utilized was a STA 449 F3 Jupiter model, from Netzsch. The essay conditions were: a temperature interval from 20 to 1200 °C with a heating rate of 20 °C min^{-1} and synthetic air atmosphere with a flux of 5 ml min^{-1}, situated in high alumina crucibles. The temperatures of glass transition (T_g), softening (T_s) and crystallization (T_c) were obtained by the first derivation method, i.e., as this temperatures are kinetic events, the first derivative on the DSC curve was used and the T_g or T_s were determined as the major peaks on the derivative curves for each glass composition. The Netzsch Proteus® software was used to accurately determine T_g and T_s.

The Fourier Transform Infrared Spectroscopy (FTIR) technique was employed to analyze the behavior of the bonds between Si–O, Al–O, Mg–O, Ca–O, Na–O and Fe–O in the vitrification of the materials studied. The device utilized was an infrared spectrophotometer from Shimadzu, model IR Prestige 21. The sample was mixed to KBr in the ratio of 1% sample to 99% KBr by volume.

Results and discussion

XRF analysis of bottom ash

Table 2 shows the chemical elements present in the composition of mineral coal bottom ash. The components, identified

by the XRF technique (Table 2) take part in the process of the acquisition of glass in different shapes. The elevated silicate percentage, for instance, justifies the employment of ash as a source material for the glass network.

Alumina, according to Navarro [14] and Harper [17] increases the chemical durability and the mechanical resistance. The iron oxide acts mainly as a dye, providing a black color (for high iron levels) or yellow color (for smaller iron quantities) to the material [18].

Titanium oxide, as stated by Varshneya [19], acts as a nucleating agent, favoring the emergence of crystals during the thermal treatment process of the crystallization.

The calcium, sodium and potassium oxides act as fusion agents and are fundamental in the production of glass. The melting agents are compounds which, when added to the glass net, decrease the melt temperature, viscosity and glass transition temperature [20]. They are mostly alkali metal oxides and act as network modifiers. Modifications in glass properties are due to loss of connectivity, transforming a covalent oxygen bond into ionic and can provide extra oxygen ions, increasing the Si/O ratio in the glass [21].

Potassium oxide, according to Navarro [14], interferes in the composition of the glass when present in amounts lower than 1.0% and given that the bottom ash contains 3.1% of K_2O. Compared to sodium oxide, potassium oxide increases the viscosity of the glass and increases its thermal range of work.

Sodium oxide (NaO) acts to reduce the viscosity of the glass, favoring its softening temperature; the cation has great affinity with oxygen, which in turn breaks its bond with silica and binds to sodium, causing a break in the net. Excess sodium in the formulation, however, renders the material soluble in water [22].

Calcium binds to the oxygen by breaking the bonds between oxygen and silica, and, because of their bivalence, each calcium atom binds to two oxygen atoms. Since it generates a new bond for every two bonds destroyed, calcium is not as efficient as sodium in reducing the softening temperature, but given its poor solubility in water, it becomes more resistant to solubility [23]. Calcium oxide in proportions greater than 46.0% in the vitreous composition does not act as a network modifier, forming Ca–O–Ca, while the majority of the calcium cations occupies CaO_6 distorted octahedra surrounded by chains of SiO_4 tetrahedra [24].

Magnesium oxide acts as a network stabilizer, lowering the dilation coefficient and increasing the resistance to thermal shock [14].

Particle size distribution

Fig. 1 presents the size distribution of the bottom ash particles *in natura* after oven drying for 24 h at 105 °C.

The bottom ash presented a greater quantity of passing particles in the 50 mesh (0.297 mm), which totalled 24.5% of the particles. The size of interest is the 200 mesh (0.074 mm), but only 4.8% of the particles presented this diameter. Such fact justified the milling of the product in order to reduce particle size and guarantee a better homogeneity of the vitreous mixture.

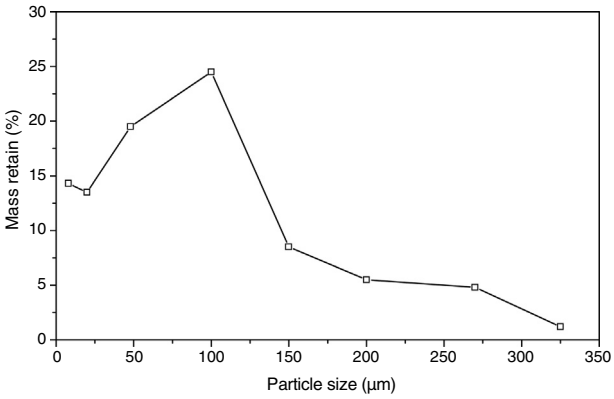

Fig. 1 – Size distribution of the bottom ash particles.

Physical characteristics of the glasses formed

Fig. 2 illustrates the glasses obtained from bottom ashes based on the experimental design.

The materials obtained exhibited the characteristics of a glass, such as high brightness (not measured). Their brittle aspect was a consequence of being poured on a cold surface, thus generating tractive tensions on the external side and compressive ones in the interior of the vitreous droplet. This problem can be bypassed with the thermal treatment of annealing for tension relief, which consists in inserting the poured vitreous piece in an oven at a low temperature. Fig. 2 presents the formed glass without undergoing any heat treatment, thus justifying the presence of cracks.

Most glasses present identical physical characteristics, hampering their differentiation without the use of characterization techniques or adequate devices. However, some samples differed from the rest, e.g. sample 9, which presented a certain opacity, a characteristic that makes glasses esthetically undesirable. Sample 9 presented different physical characteristics compared the other glasses. As verified in the XRD technique, this material formed crystalline phases, not characterizing it as glass. Its composition presents 45.8% of sodium carbonate or, if neglecting the CO_2, 26.8% of NaO. The sample also presented a high content of CaO and MgO (11.0% and 5.5%, respectively), oxides which are crystalline structure builders. Sodium reduces the viscosity of the vitreous medium, increasing the mobility of crystals and the crystallization tendency. Crystallization can be defined as the process by which a stable solid phase forms from a structurally disordered phase, resulting in a geometric ordering of the structure [25]. This process occurs because the vitreous substances have lower stability than the crystalline phase, with an energetic content greater than thermodynamic equilibrium. Thus, when subjected to favorable conditions, there is a reduction of the free energy of the system, which leads to the formation of crystalline structures [14].

Bottom ash has in its composition a nucleating agent, TiO_2, which accelerates the nucleation process even in small quantities [26]. Thus, the composition of the ash and the proportions of the oxides used in the sample 9 exerted great influence on its crystallization. It can also be stated that a similar process occurred with sample 2.

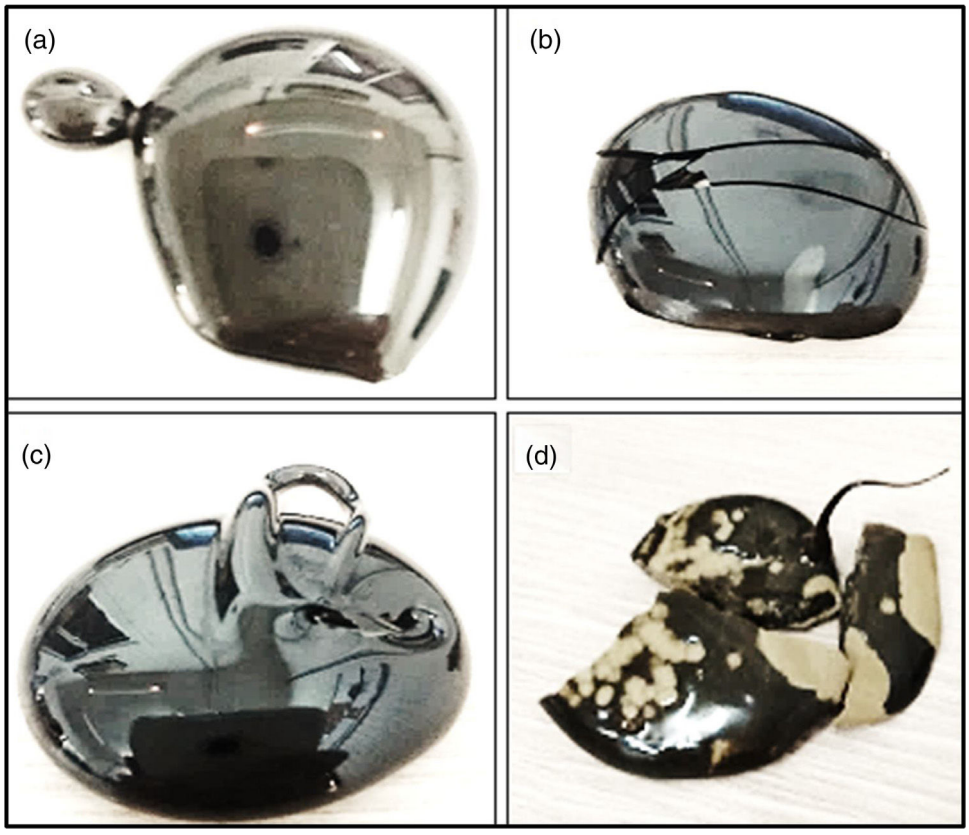

Fig. 2 – Formed glasses. Formulation 3 (a), formulation 5 (b), formulation 8 (c) and formulation 9 (d).

XRD analyses of the glasses

The diffractograms of samples 1, 3, 4, 5, 6, 7, 8 and 10 were considered amorphous and are shown in Fig. 3. The absence of well defined peaks denotes the disordered structure of the samples, which is typical of the glasses. Samples 2 and 9 exhibited typical peaks of the crystal structures (Fig. 4a and b). Peak identification was performed using the High Score PAnalytical software, according to JCPDS.

The diffractograms of the samples 2 and 9 show the formation of well defined peaks in the region of $2\theta = 21$, 35, 50 and 62°, identified as (A): $NaAlSiO_4$ (JCPDS 01-076-0909), (B): Fe_2SiO_4 (JCPDS 01-083-1654), (C): Fe_2O_3 (JCPDS 01-084-0311), (D): $Na_2Mg_2Si_2O_7$ (JCPDS 00-053-0626).

Analysis obtained through the DSC technique

DSC/TG analyses were performed for the 10 glass samples. Table 3 and Fig. 5 present the results obtained.

It is important to emphasize that the exothermic peaks (Fig. 5) are associated to devitrifications, indicating a tendency of crystallization for the formed glasses.

The formation of crystalline phases for glasses 2 and 9, confirmed by the absence of peaks, altered the thermal behavior during the DSC analysis. Glasses 2 and 9 did not clearly show a transition in glass, a typical feature of vitreous materials. However, since the DSCs showed a discrete transition of the thermal behavior associated with a T_g region, it is possible that the vitreous systems have formed ceramic eyeglass frames.

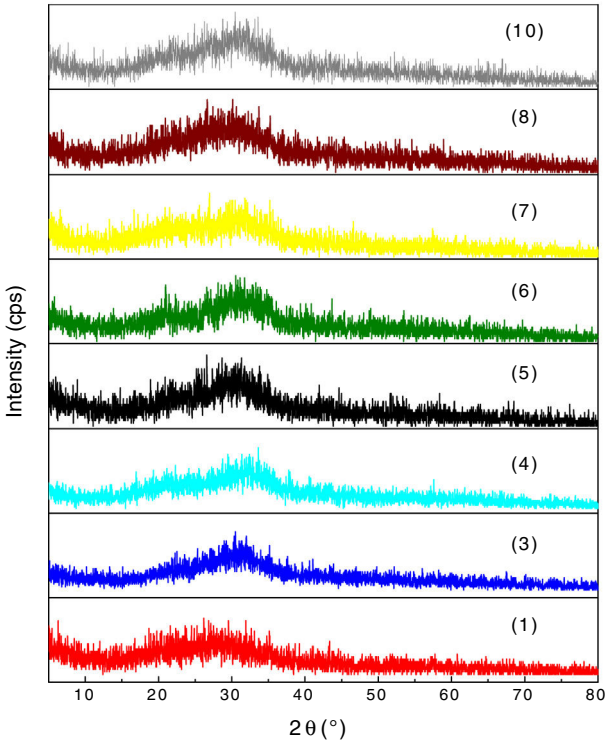

Fig. 3 – Diffractograms identified for the samples 1, 3, 4, 5, 6, 7, 8 and 10.

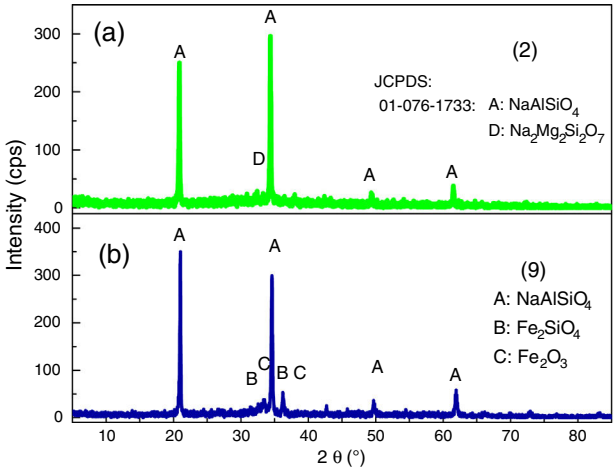

Fig. 4 – Diffractograms identified for glasses 2 and 9.

Table 3 – Glass transition (T_g), softening (T_s) and crystallization (T_c) temperatures obtained by the first derivation method by DSC.

Samples	T_g (°C)	T_s (°C)	T_c (°C)
1	579	1094	817
2	726	1060	–
3	631	1046	–
4	505	1002	567–605
5	613	1078	931
6	574	1100	766
7	537	1104	832
8	598	1151	978
9	579	1187	1127
10	571	1137	712

This is a consequence of rapid crystallization due to the higher CaO/MgO content and the presence of TiO_2 in the compositions. For the crystallization of the species – SiO_2, MgO, CaO – it is necessary that the system presents mobility for the formation of the coordination polyhedron. The low viscosity contributes to the increase of ion mobility and is related to the higher proportion of Na_2O. For the formation of crystals, crystallization nuclei must initially be formed, that is, they need a stable surface, because at high temperature all the glass is a fluid. TiO_2 acts as a nucleating agent and is a stable center for crystal growth.

Statistical analysis

In this work, the most important parameters were the glass transition (T_g) and softening (T_s) temperatures, considering the statistical analysis. As the aim of the work was to develop a suitable glass formulation for an industrial application, the lower temperatures were considered as the most adequate for energy saving during the glass melting process. Therefore, the effects that the factors (bottom ash, sodium carbonate and calcium oxide/magnesium oxide contents) exert on the characteristic temperatures (system response) were analyzed.

For a confidence interval of 95%, the quadratic model was the most significant for the T_g results and the linear model was the most significant for the T_s results. Only the main factors A, B and C (standing for bottom ash, Na_2CO_3 and CaO/MgO, respectively) were significant in the response regarding the glass transition temperature and the softening point. The Pareto diagrams (Fig. 6 and Fig. 7, respectively) show these results.

The Pareto diagram for the glass transition temperature (T_g) shows that the amount of CaO/MgO was the most important factor in order to increase the T_g, followed by the bottom ash content and the Na_2CO_3 content. The results are shown as the 'standardized effects estimate' in 'absolute values', which means the size of the effect of a given response, no matter its unit. That is, for the glass transition temperature, the amount of CaO/MgO and bottom ash are the parameters which show the greatest influence on the T_g results regarding the size of the effect, not on the value of the glass transition temperature.

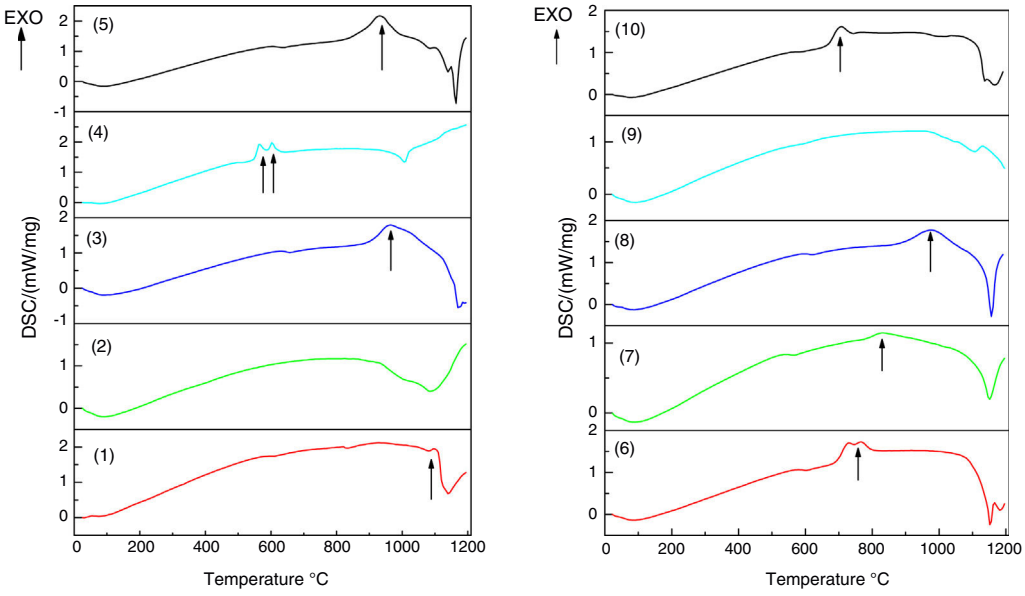

Fig. 5 – Graphs of differential scanning calorimetry (DSC) technique for samples 1–10.

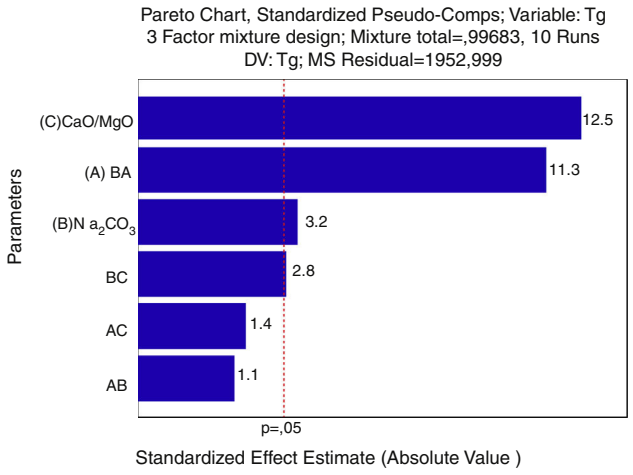

Fig. 6 – Pareto diagram for T_g.

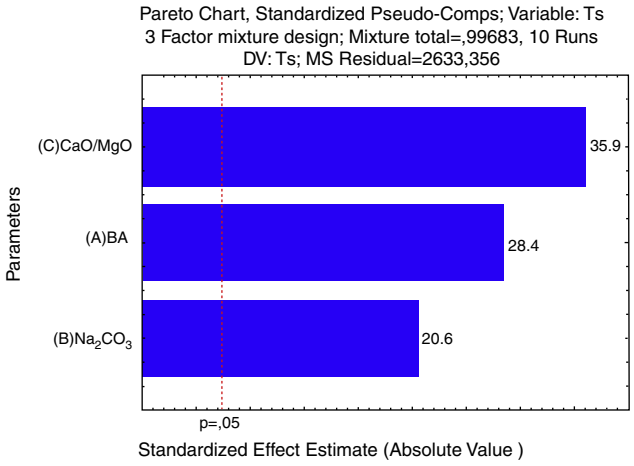

Fig. 7 – Pareto diagram for T_s.

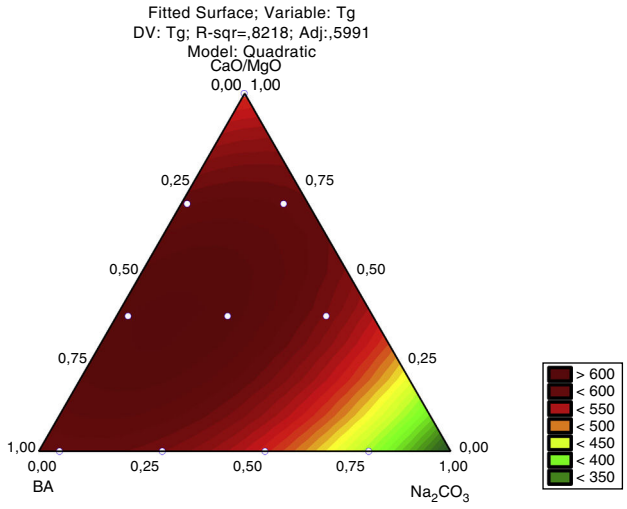

Fig. 8 – Response surface graph for T_g.

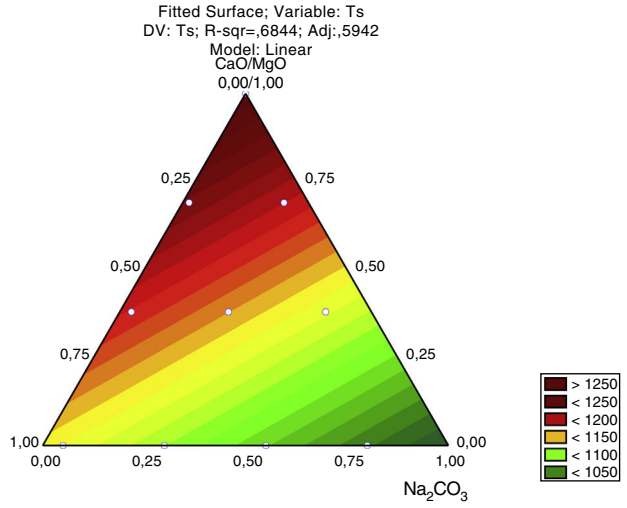

Fig. 9 – Response surface graph for T_s.

Regarding the softening temperature, the Pareto diagram (Fig. 7) shows the same trend as for the glass transition temperature. The amount of CaO/MgO was the most significant factor to increase the softening temperature, followed by the amount of bottom ash and the amount of Na_2CO_3. For the T_s, the Pareto chart shows that all the three parameters are very significant regarding the 95% confidence interval. The degree of significance for both T_g and T_s is 0.997, meaning a confidence of 99.7%.

The response surface for the glass transition temperature, Fig. 8, shows that the lowest T_g are achieved when the amount of Na_2CO_3 is increased in the glass formulation. The Na_2CO_3 brings Na_2O to the structure of the silica glass, a strong modifier that raises the number of non-bridging oxygen and therefore weakens the glass structure. The bottom ash alone raises the T_g due to its chemical composition, mainly SiO_2, a glass former, and Al_2O_3, also a glass former when in tetrahedral coordination. CaO and MgO also raise the T_g. This is due the valence of each ion, Ca^{2+} and Mg^{2+} cause a lower reduction in the bonding energy of the silica glass (Si^{4+} and Al^{3+}) than the Na^+ ions. Regarding the Pareto chart, the CaO/MgO amount causes a stronger effect on T_g due to the size effect, but not in the decrease of the glass transition temperature. This effect is probably due to the addition of Na^+ ions to the glass compositions in the form of a carbonate (Na_2CO_3), and not as a pure oxide like the CaO/MgO mixture.

For the softening temperature (T_s), Fig. 9, the effect of the amount of Na_2O is stronger than in the glass transition temperature (T_g) and its size effect, given by the Pareto chart (Fig. 6) is like the size effect of the other raw materials (bottom ash and CaO/MgO). The CaO/MgO addition strongly raises the softening temperature, while the bottom ash has an intermediate effect. The amount of bottom ash used in this study – 78.0 to 53.3% – was probably just enough to form the glass structure, indicating that the amount of CaO/MgO is in excess, thus raising the bonding energy. But this is only an assumption, since NMR studies are needed to give the speciation of the O (bridging and non-bridging) and Si ions in the glass structure.

FTIR analysis performed on the glasses

Fig. 10 shows the results of the FTIR analysis performed in the ten samples of synthesized glasses.

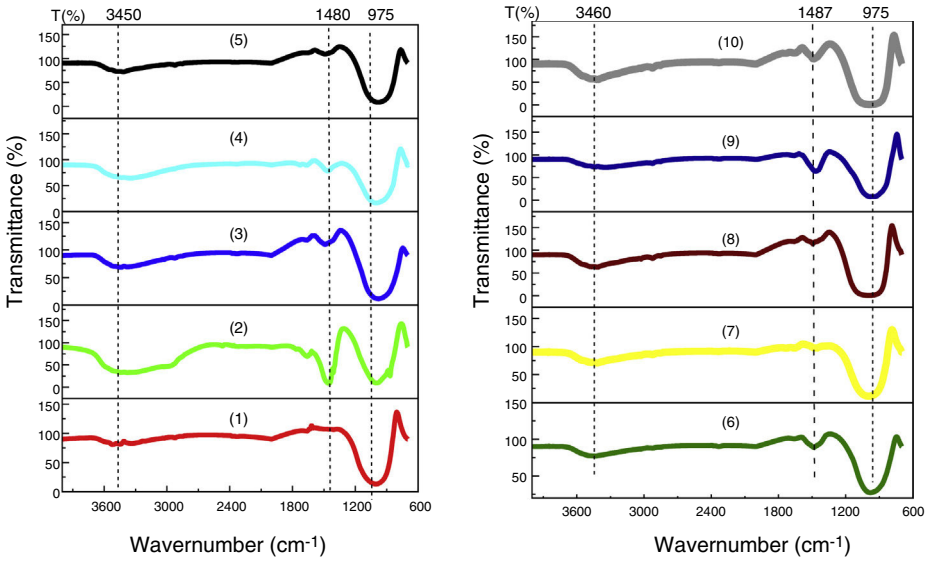

Fig. 10 – FTIR for the ten glass samples.

In every specter (Fig. 10), three regions can be distinguished, each characterized by absorption maxima due to different types of vibration:

(a) 950–1200 cm^{-1}, represent stretching vibrations of Si–O–Si and Si–O–M (M = A1, Mg, Fe) [27].
(b) 1460–1500 cm^{-1}, represent stretching vibrations of carbonation (CO_3) [28,29], probably due to atmospheric contamination, since the decarbonation process occurs around 850 °C.
(c) 3450–3670 cm^{-1}, the bands between 3450 and 3670 cm^{-1} are attributed to the stretching of OH [30]. The identified OH group has the same origin as CO_2, i.e., the water identified in this analysis comes from environmental contamination.

Conclusion

The attainment of glass from bottom ash was viable and completely satisfactory, since the raw material employed is considered a residue, which if not utilized can become an environmental problem due to its careless disposal in the environment.

The XRD analyses showed that, out of the ten formulations tested, only two did not form glasses, but crystals; both differed from the rest in the color and the brightness (opaque) of the piece. For the crystalline samples, one phase was identified for Glass 2 ($NaAlSiO_4$) and three for Glass 9 ($NaAlSiO_4$, Fe_2O_3 and Fe_2SiO_4). The crystallization occurred in glasses with a low content of bottom ash (58.5 and 56.7%) and melting agents (41.5 and 43.3%), mainly NaO, which decreases the viscosity of the medium and favors the mobility of the ions, thus increasing the tendency of forming crystals. The presence of TiO_2 in the bottom ash composition favored the formation of crystals, since this oxide is a nucleating agent.

The DSC analyses showed that the vitreous mixtures melt at temperatures below 1500 °C, which is due to the effect of the melting agents. Pure bottom ash melts at a much higher temperature, evidencing thus an energy economy, in addition to improving the properties of the material. The lowest softening temperature was observed in Glass 4 (65.0% bottom ash, 47.3% Na_2CO_3 and 7.3% CaO/MgO), which was 1002 °C and the highest in Glass 8 (69.3% bottom ash, 24.2% Na_2CO_3 and 16.5% CaO/MgO), this being 1151 °C. In the TG analysis, no loss of mass of the obtained materials was evidenced. In addition, the DSC analysis showed that all the glasses of the formulation exhibited exothermic peaks, indicating a tendency to crystallize the samples. The absence of peaks was shown for already crystallized samples.

According to the statistical analysis, the raw materials exerted a great influence on both the softening (T_s) and glass transition (T_g) temperatures, in which CaO/MgO fluxes followed by bottom ash were the factors that most contributed to their growth. The presence of sodium oxide decreased T_g and T_s. CaO/MgO caused a lower reduction of the vitreous bond energy when compared to NaO, which in turn is the most influent factor in the glass transition and softening temperatures.

FTIR analyses ascertained the existence of the probable elements present in the glass samples, evidencing the Si–O and Si–O–M (M = A1, Mg, Fe) bonds, stretching vibrations of carbonation (CO_3) and OH vibrations, the two latter being considered contamination by the external environment.

Acknowledgments

The authors wish to thank Tractebel Energy and UFSC for the support in this research.

REFERENCES

[1] Plano Nacional de Energia, 2030: Geração termoelétrica: carvão mineral, 2007.

[2] World Coal Association. Available from: https://www.worldcoal.org/.
[3] L. Bartoňová, Unburned carbon from coal combustion ash: an overview, Fuel Process. Technol. 134 (2015) 136–158.
[4] M. Rafieizonooz, J. Mirza, M.R. Salim, M.W. Hussin, E. Khankhaje, Investigation of coal bottom ash and fly ash in concrete as replacement for sand and cement, Constr. Build. Mater. 116 (2016) 15–24.
[5] Eletric Power Research Institute, Coal Ash: characteristics, management and environmental issues, EPRI Report 1019022, September, 2009.
[6] S.S.G. Hashemi, H.B. Mshmud, J.N.Y. Djobo, C.G. Tan, B.C. Ang, N. Ranjbar, Microstructural characterization and mechanical properties of bottom ash mortar, J. Clean. 170 (2018) 797–804.
[7] M. Erol, S. Kuçukbayrak, A. Ersoy-Meriçboyu, Characterization of coal fly ash for possible utilization in glass production, Fuel 86 (2007) 706–714.
[8] American Coal Ash Association (CAAA), Coal ash production, use survey 2014, News Conference – Washington, D.C., American Coal Ash Association (CAAA), Coal ash production and use survey 2014, News Conference – Washington DC, 2015. Available from: https://www.acaa-usa.org/Portals/9/Files/PDFs/2014-Production-and-Use-Survey-Presentation.pdf.
[9] R.A.A. Boca Santa, C. Soares, H.G. Riella, Geopolymers obtained from bottom ash as source of aluminosilicate cured at room temperature, Constr. Build. Mater. 157 (2017) 459–466.
[10] F.E. Huggins, Overview of analytical methods for inorganic constituents in coal, Int. J. Coal Geol. 50 (2002) 169–214.
[11] H.K. Kim, Utilization of sieved and ground coal bottom ash powders as a coarse binder in high-strength mortar to improve workability, Constr. Build. Mater. 91 (2015) 57–64.
[12] U. Ulusoy, C. Igathinathane, Particle size distribution modeling of milled coals by dynamic image analysis and mechanical sieving, Fuel Process. Technol. 143 (2016) 100–109.
[13] M. Akerman, Introdução ao vidro e sua produção, ABIVIDRO – Escola do Vidro, 2013.
[14] J.M.F. Navarro, El vidrio, 3 ed, Consejo Superior de Investigaciones Científicas, Madrid, 2003.
[15] C. Choi, S. Kang, Crystallization behavior at nucleation sites on the surfaces of vitreous materials loaded with coal bottom ash, J. Korean Phys. Soc. 54 (2009) 1320–1324.
[16] W. Kim, S. Kang, Processing research influence of TiO_2 additions on the crystallization kinetics of a coal bottom ash-Li_2O glass system, J. Ceram. Process. Res. 11 (2010) 557–560.
[17] C.A. Harper, Handbook of Ceramics, Glasses and Diamonds, McGraw-Hill, 2001.
[18] C.T. Kniess, N.C. Kuhnen, H.G. Riella, E. Neves, C.D.G. Borba, Estudo do efeito da quantidade de óxido de ferro em cinzas pesadas de carvão mineral na obtenção de vitrocerâmicos, Quim. Nova 25 (2002) 926–930.
[19] A.K. Varshenya, Fundamentals of Inorganic Glasses, Academic Press, Inc., New York, 1994.
[20] Y.M. Chiang, P.D. Birnie, W.D. Kingery, Physical Ceramics: Principles for Ceramic Science and Engineering, 1st ed., John Wiley & Sons, New York, 1997.
[21] J. Zarzycki, Les verres et l'état vitreux, Manson, Paris, 1982.
[22] L. Fugita, Utilização de selênio como colorante/descolorante em vidros sodo-cálcicos, EPUSP, São Paulo, 2004.
[23] M. Akerman, Natureza, estrutura e propriedades do vidro, 2000.
[24] D.S. Meneses, M. Malki, P. Echegut, Optical and structural properties of calcium silicate glasses, J. Non-Cryst. Solids 352 (2006) 5301–5308.
[25] W. Höland, G. Beall, Glass-ceramics Technology, The American Ceramics Society, Westerville, 2002.
[26] Z. Strnad, Glass-ceramic Materials, Elsevier, Amsterdam, 1986.
[27] M.A. Karakassides, An infrared reflectance study of Si–O vibrations in thermally treated alkali-saturated montmorillonites, Clay Miner. 34 (1999) 429–438.
[28] E. Arioz, O. Arioz, O.M. Kockara, Leaching of F-type fly ash based geopolymers, Proc. Eng. 42 (2012) 1114–1120.
[29] I. Lancellotti, M. Cannio, F. Bollino, M. Catauro, L. Barbieri, C. Leonelli, Geopolymers: an option for the valorization of incinerator bottom ash derived "end of waste", Ceram. Int. 41 (2015) 2116–2123.
[30] B.J. Saikia, G. Parthasarathy, Fourier transform infrared spectroscopic characterization of kaolinite from Assam and Meghalaya, Northeastern India, Int. J. Mod. Phys. 1 (2010) 206–210.